Polyhedron 133 (2017) 358–363

Contents lists available at ScienceDirect

Polyhedron

journal homepage: www.elsevier.com/locate/poly

“Tetramethylsilanoviologen”: Synthesis, characterization, and hydrolysis of a Silolodipyridinium ion

David A. Lee, Derek M. Peloquin, Edi W. Yapi, Lucas A. McMinn, Jon W. Merkert, Bernadette T. Donovan-Merkert, Ashley Ariel Vitallo, Ashley R. Peterson, Daniel S. Jones, Christopher Ceccarelli, Thomas A. Schmedake *

University of North Carolina – Charlotte, Department of Chemistry, Charlotte, NC 28223, USA

ARTICLE INFO

Article history:
Received 4 April 2017
Accepted 23 May 2017
Available online 31 May 2017

Keywords:
Hexacoordinate silicon
Bipyridine
Coordination chemistry
Electrochemistry
Crystallography

ABSTRACT

A silicon-bridged viologen has been synthesized by methylation of 4,4′-dipyridinodimethylsilole, and represents a new addition to the growing family of heteroatom bridged viologens. The dicationic species emits at 360 nm and exhibits two chemically reversible one electron reduction waves in acetonitrile at $E_{1/2}(2+/1+) = -0.829$ V and $E_{1/2}(1+/0) = -1.307$ V (versus Fc/Fc^+). The UV–Vis spectrum for each of the three charge states is similar to the corresponding unbridged methyl viologen species. The silanoviologen is susceptible to ring-opening hydrolysis.

1. Introduction

The N-alkylated 4,4′-bipyridininium salts (viologens) have been widely adopted as redox active components in a diverse array of applications such as electron mediators for hydrogen generation [1], electrochemical capacitors [2], and electrochromic displays [3]. The 4,4′-bipyridinium di-cations can be readily reduced to form relatively stable radical cation species [4] with intense colors that vary with the N-substituent. Likewise, metalloles including siloles and dibenzosiloles constitute an important class of materials with extensive academic interest and practical applications, including luminescent devices [5], photovoltaics [6], and sensors for explosives [7]. Siloles are electron acceptors due to contribution of the silicon σ^* orbitals to the LUMO of the sila-cyclopentadiene ring, and there has been extensive interest in incorporating fused siloles and other metalloles into polymers and extended conjugated systems [8]. Ohshita and coworkers synthesized the first 4,4′-dipyridinosilole and explored its solid state luminescence [9], but N-alkylation to make the silicon bridged viologen has not yet been reported.

Synthetic modification at the C3 position of 4,4′-bipyridinium salts is usually undesirable since it prevents planarity and destabilizes the reduced species. C3-C3′ bridging substituents on the other hand enforce planarity and are an attractive synthetic target for tailoring the chemical, electrochemical, and optical properties of the viologens. Heteroatom bridged methyl viologen analogs have appeared in the literature with N, P, S, and Ge bridges (Scheme 1), with various effects attributed to the heteroatom incorporation. The 9-oxide-9H-phospholodipyridinium salts, e.g. **P-MV**, exhibit significantly lowered reduction potentials thanks to the phosphine oxide bridge [10]. This could enable sensing or catalytic applications involving electron transfer from weaker electron donors. Phosphaviologens have also been explored as tunable electrochromic materials [11]. The 2,7-dimethylthieno[2,3-c:5,4-c′] dipyridinium ion, **S-MV**, was shown to act as an electron shuttle and a photosensitizer for the photoreduction of water [12]. By comparison, unbridged methyl viologen can only act as an electron shuttle for the photoreduction of water in the presence of a photosensitizer such as $Ru(bpy)_3^{2+}$. Pyrrolodipyridinium salts such as **N-MV** were developed for potential cytostatic activity [13]. A germanium bridged analog, **Ge-MV**, was recently synthesized, and it was shown that the germanium bridge slightly increased the electron affinity of the viologen with a slight shift of +0.08 V relative to methyl viologen’s first reduction potential [14].

Silicon bridged viologens would be an attractive addition to this family combining benefits of siloles and viologens, and the silicon bridge could also enforce planarity while providing a useful site for subsequent functionalization or immobilization. Immobilization of viologens [15] on surfaces has proven beneficial, for example, in

---

* Corresponding author.
E-mail address: tschmeda@uncc.edu (T.A. Schmedake).

http://dx.doi.org/10.1016/j.poly.2017.05.040
0277-5387/

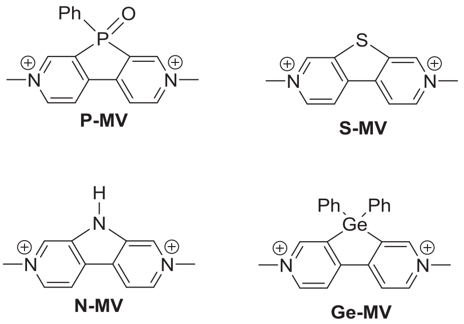

Scheme 1. Previously reported heteroatom bridged methyl viologen analogs, **P-MV**, **S-MV**, **N-MV**, and **Ge-MV**.

electrochromic device applications [16] and renewable carbohydrate fuel cells [17]. In this manuscript, we report the synthesis and structural characterization of a silanoviologen and explore its electrochemical, electrochromic, and hydrolytic stability.

2. Results and discussion

The precursor, 4,4′-dipyridinodimethylsilole, **1**, was synthesized by allowing dichlorodimethylsilane to react with Li_2bipy at 85 °C following the method of Ohshita (Scheme 2). Subsequent chromatography and recrystallization from hexane provided a colorless crystalline material in 49% yield. Single crystals suitable for X-ray analysis were obtained via slow evaporation from hexane. The crystal structure of **1** is shown in Fig. 1.

Crystals of **1** were subsequently dissolved in acetonitrile and methylated with methyl triflate to produce the tetramethylsilanoviologen, **2**. Colorless crystals of **2** were recovered from the reaction mixture in 61% yield by diffusion of ether into the solution. The crystal structure of **2** is shown in Fig. 2 with anions and solvent omitted for clarity. Both structures exhibit a nearly planar bipyridinium framework with a small value for the C1–Si–C10 bond angle of 90.09(8)° for **1** and 88.55(11)° for **2**.

The dimethylsilylene bridge has a subtle effect on the spectroscopic properties of the methyl viologen analog. A deoxygenated acetonitrile solution of compound **2** absorbs in the UV with a $\lambda_{max} = 270$ nm and emits with a broad emission band centered at 360 nm (Fig. 3). Both values are only slightly lower in energy than those reported for methyl viologen 260 nm [18] and 350 nm [19], respectively.

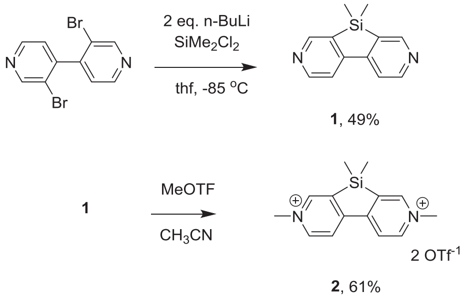

Scheme 2. Synthesis of **1** and **2**.

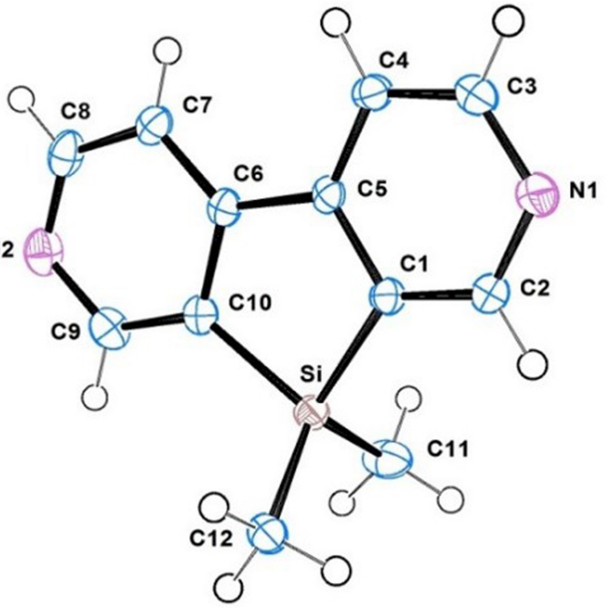

Fig. 1. Crystal structure of **1**. Selected bond distances (Å) and angles (°): Si–C1 1.8801(18), C1–C5 1.408(2), C5–C6 1.485(2), C6–C10 1.411(2), C10–Si 1.8858(18), C1–Si–C10 90.09(8), Si–C1–C5 110.27(13), C1–C5–C6 114.78(15), C5–C6–C10 114.71(15), C6–C10–Si 110.04(13). Torsion angles (°): C1–C5–C6–C10 0.2(2), Si–C1–C2–N1 −178.12(15).

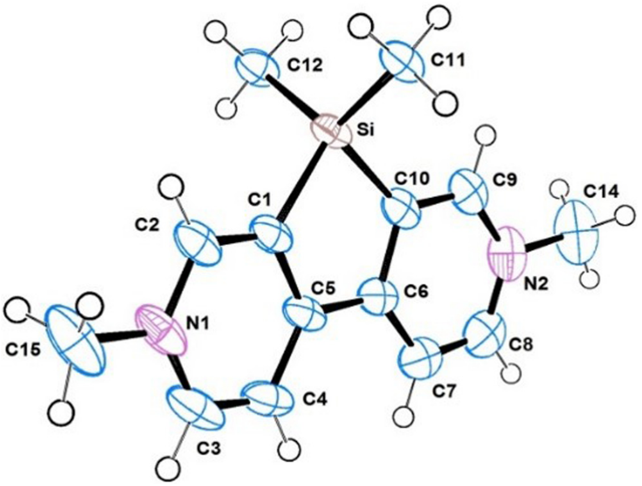

Fig. 2. Crystal structure of **2**. Counterions (two triflate ions) and solvent molecules omitted for clarity. Selected bond distances (Å) and angles (°): Si–C1 1.889(2), C1–C5 1.402(4), C5–C6 1.484(4), C6–C10 1.406(4), C10–Si 1.889(2), C1–Si–C10 88.55(11), Si–C1–C5 111.30(18), C1–C5–C6 114.5(2), C5–C6–C10 113.8(2), C6–C10–Si 111.74(19). Torsion angles (°):C1–C5–C6–C10 −1.2(3), Si–C1–C2–N1 −179.74(18).

The effect of the dimethylsilylene bridge on the reduction potentials is also subtle. The standard reduction potentials of **2** were determined via cyclic voltammetry in acetonitrile solution with tetra-n-butylammonium hexafluorophosphate (0.10 M) as the electrolyte (Fig. 4). A platinum disk working electrode was used along with a Ag/AgCl reference electrode and the ferrocene/ferrocenium couple was used as an internal standard. The silanoviologen dication exhibits two chemically reversible one electron reduction waves at $E_{1/2}(2+/1+) = -0.829$ V and $E_{1/2}(1+/0) = -1.307$ V (versus Fc/Fc^+), very similar to values reported for **Ge-MV** of $E_{1/2}(2+/1+) = -0.80$ V and $E_{1/2}(1+/0) = -1.25$ [14].

The UV–Vis spectra of the 1 + and neutral reduced states of **2** were obtained using an argon flushed spectroelectrochemical cell with a 1.0 mm pathlength and a printed gold honeycomb working electrode (Pine Instruments), a gold counter electrode, and a Ag/AgCl reference electrode standardized to the ferrocene/ferrocenium couple. Dilute samples of **2** were prepared in anhydrous acetonitrile with tetra-n-butylammonium hexafluorophosphate (0.1 M). Figs. 5 and 6 contain the spectra of the 2 + species (red),

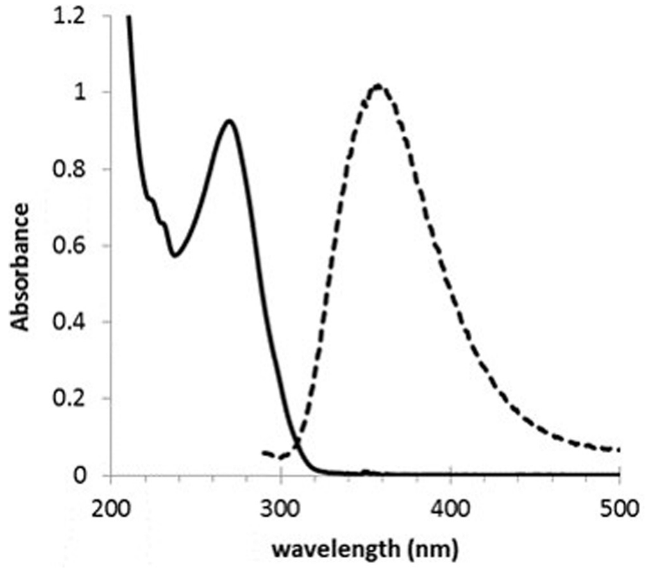

Fig. 3. UV–Vis (solid line) and fluorescence (dashed line) spectra of **2** in degassed CH_3CN solution.

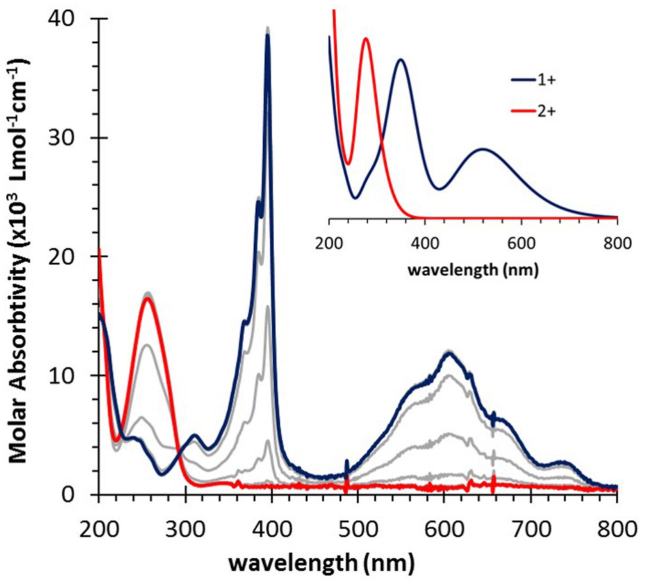

Fig. 5. UV–Vis spectra of $\mathbf{2}^{n+}$ states generated electrochemically at −0.695 V (red line, $n = 2$), −1.095 mV (blue line, $n = 1$), and at 50 mV intervals (grey). Simulated spectra of $\mathbf{2}^{2+}$ and $\mathbf{2}^{1+}$ are also included (insert). (Color online.)

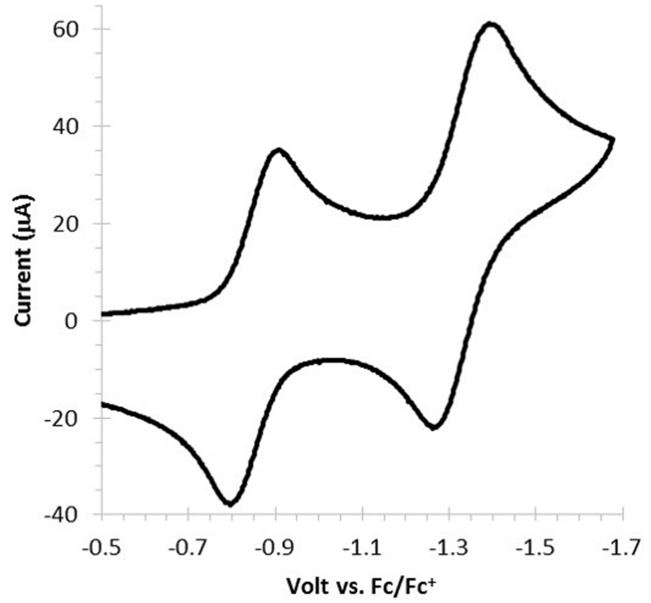

Fig. 4. CV of scan of **2** in acetonitrile with $N(n\text{-}Bu)_4PF_6$ (0.10 M) as supporting electrolyte. Scan rate = 200 mV/s with iR compensation.

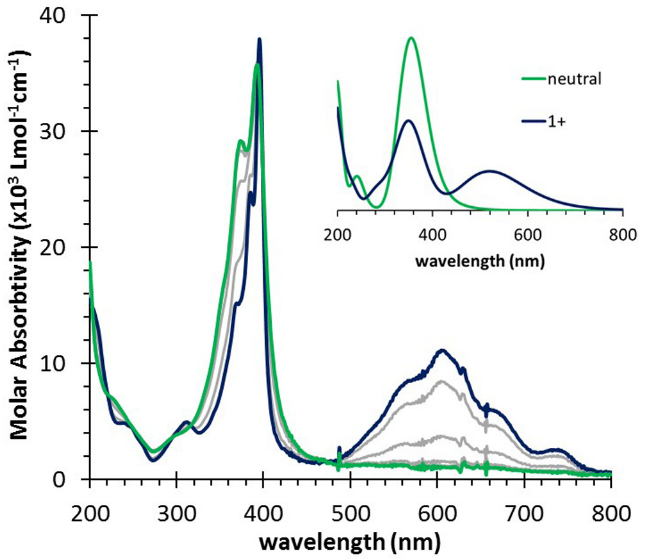

Fig. 6. UV–Vis spectra of $\mathbf{2}^{n+}$ states generated electrochemically at −1.095 V (blue line, $n = 1$), −1.445 V (green line, $n = 0$). Simulated spectra of $\mathbf{2}^{1+}$ and neutral **2** (insert). (Color online.)

1 + species (blue), and neutral species (green) obtained at working electrode potentials of −0.695 V, −1.095 V, and −1.445 V respectively versus Fc/Fc+. Additional spectra were taken at 0.050 V intervals (grey) to indicate isosbestic points for each transition. The observed spectra match up reasonably well with simulated spectra calculated using time dependent density functional theory (Figs. 5 and 6 inserts) and are very similar to the corresponding unbridged methyl viologen spectra. Details of spectra simulations are included in the ESI.

The spectroscopic properties of **2** are more consistent with the properties of a methyl viologen than the properties of a silole. The explanation for this can be seen in the DFT calculated LUMOs of three heteroatom bridged viologens, **2**, **P-MV**, and **Ge-MV** (Fig. 7). The LUMO of **2** is localized on the viologen framework, while the silole-like contribution of the exocyclic silicon σ^* orbitals to the sila-cyclopentadiene ring is relegated to the LUMO + 1 (1.3 eV higher in energy than the LUMO, see ESI). Furthermore, the calculated LUMO energies of the three heteroatom bridged viologens correlate strongly with the experimentally observed reduction potentials (Fig. 8).

During our initial attempts to methylate **1**, methyl iodide was used as the methylating agent. Addition of methyl iodide to a solution of **1** in CD_3CN resulted in a red precipitate and an NMR spectrum consistent with the desired silanoviologen. The intense color of the compound was attributed to charge transfer with the iodide counter ion. Slow evaporation of the supernatant in air afforded crystals suitable for X-ray analysis. The structure was found to be that of the hydrolyzed compound (Fig. 9), indicating a significant increase in hydrolytic susceptibility upon alkylation. The increased hydrolytic susceptibility of the silanoviologen was unexpected since **1** is not observed to undergo hydrolysis in the presence of

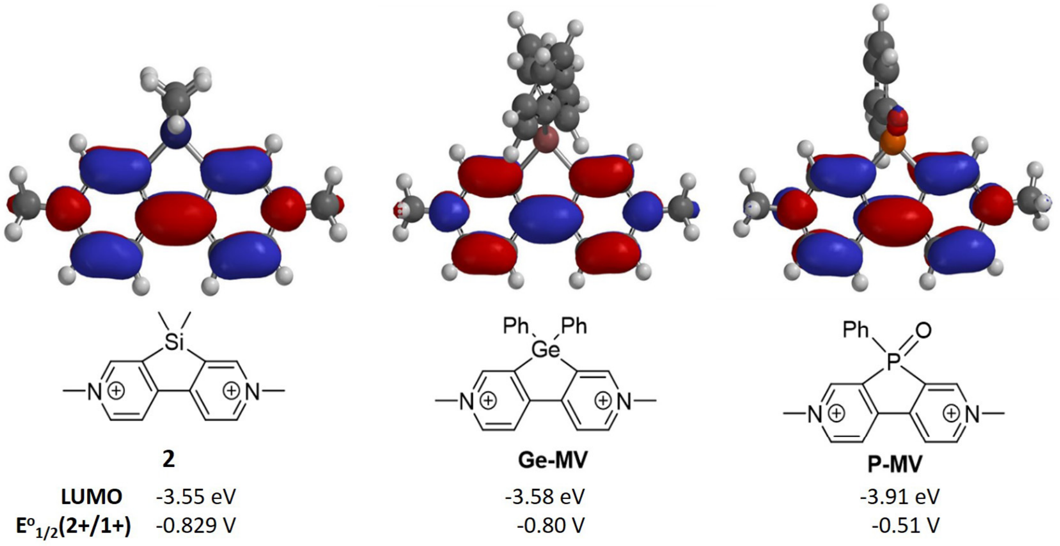

Fig. 7. LUMOs of heteroatom bridged methyl viologens calculated using density functional theory using B3LYP/6-31G(D) and Conductor-Like Polarizable Continuum Model (CPCM, dielectric = 37.22) along with first reduction potentials reported in volts vs. Fc^+/Fc for **2**, **Ge-MV**,[14] and **P-MV**.[10]

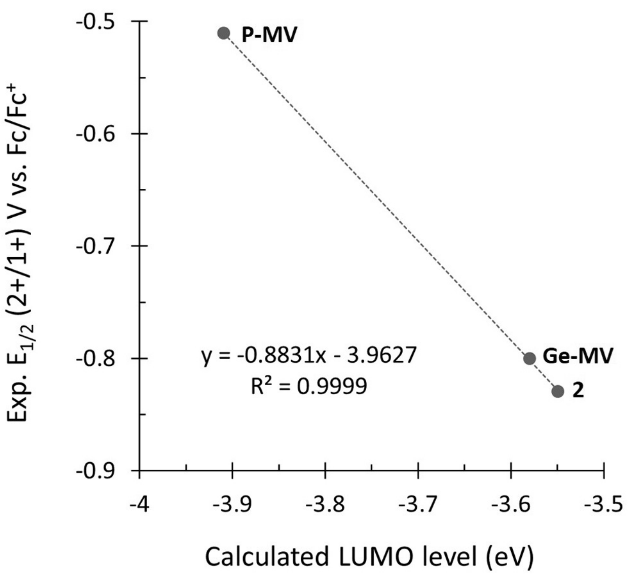

Fig. 8. Graph of first reduction potential $E_{1/2}(2+/1+)$ of heteroatom bridged methyl viologens vs. calculated LUMO level.

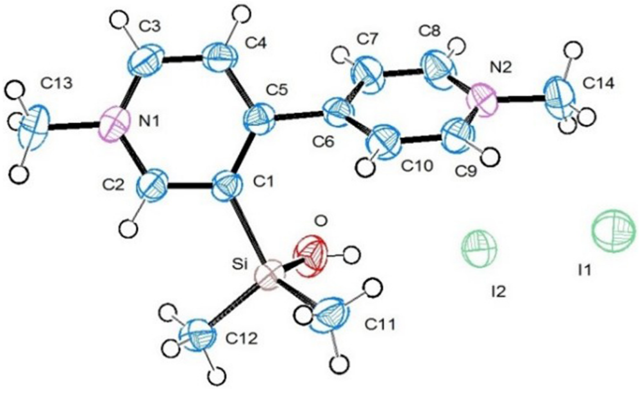

Fig. 9. Crystal structure of **3**. Selected bond distances (Å) and angles (°): Si–C1 1.922 (2), C1–C5 1.405(3), C5–C6 1.486(3), C6–C10 1.389(3), O–Si–C1 103.18(11), Si–C1–C5 125.77(17), C1–C5–C6 121.5(2), C5–C6–C10 120.6(2), C6–C10–Si 111.74(19). Torsion angle (°):C1–C5–C6–C10 −54.5(3).

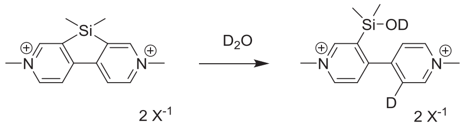

2

3

Scheme 3. Hydrolsyis of **2**.

water. However, the increased reactivity is rationalized by assuming the cationic N-methylpyridinium makes a much better leaving group than the neutral pyridine. To further explore the hydrolysis reaction, a solution of **2** (initial concentration of 38 mM) in D_2O was maintained at 23 °C and monitored by ^1H NMR at 20 min intervals. A clean conversion of **2**–**3** (Scheme 3) was observed with a rate constant of $2.3 * 10^{-4}\ M^{-1}\ s^{-1}$, which corresponds to a half-life of 72 min at 23 °C for compound **2** in D_2O (Fig. 10).

3. Conclusion

The 2,7,9,9-tetramethylsilolo[2,3-c:5,4-c′]dipyridinium ion has been synthesized and is the first reported example of a silanoviologen. The incorporation of a silylene bridge at the 3,3′-position of a 4,4′-bipyridinium ion has a subtle effect on the electronic and electrochromic properties of the compound, comparable to that of a germanium bridge, and could be a potential site for anchoring the viologen to an electrode, chromophore, catalyst, nanoparticle, or other substrate. However, the silanoviologen is susceptible to ring opening hydrolysis, which is likely to prevent its use in aqueous based applications such as hydrogen generation. It is possible that bulkier substituents on silicon could kinetically stabilize the silanoviologen with respect to hydrolysis, which will be the subject of further study.

4. Experimental

4.1. Instrumentation and general methods

Absorption spectra were measured with a Cary 300 UV–Vis spectrophotometer. Spectroelectrochemical measurements were

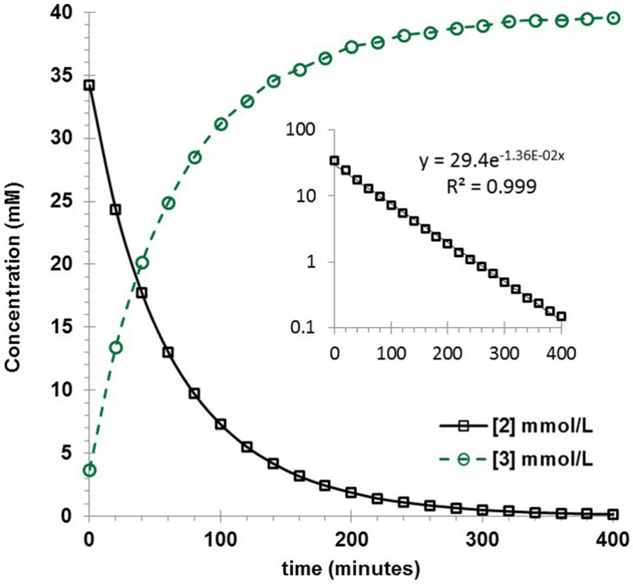

Fig. 10. Hydrolysis of **2**–**3** in D_2O. Inset shows semi-log plot of [**2**] over time.

made with an Agilent 8453 diode array UV–Vis spectrophotometer in a Pine Research Instrumentation honeycomb spectroelectrochemical cell. Fluorescence measurements were conducted on a Jobin-Yvon Fluorolog 3 fluorescence spectrometer. ^1H and ^{13}C NMR spectra were acquired using a JEOL 300 MHz NMR spectrometer. For the [29] Si spectra a JEOL 500 MHz NMR spectrometer was used. Combustion analysis (C, H, and N) was conducted by Atlantic Microlab, Inc.

Cyclic voltammetry studies were performed using a Princeton Applied Research Model 273A Potentiostat/Galvanostat employing a conventional three-electrode setup consisting of a platinum disk or glassy carbon working electrode, a silver/silver chloride reference electrode, and a platinum wire auxiliary electrode. Positive feedback iR compensation was routinely used. Voltammograms were obtained in 0.1 M tetrabutylammonium hexafluorophosphate ($TBAPF_6$)/acetonitrile solution using solvent that had previously been purified and dried using a solvent purification system (SPS-400, Innovative Technologies) and subsequently purged with nitrogen. The supporting electrolyte ($TBAPF_6$) was recrystallized from ethanol and dried under vacuum prior to use. Ferrocene was used as an internal standard without further purification.

X-ray crystallographic data was acquired with an Agilent Gemini A Ultra diffractometer. Crystals of suitable size were coated with a thin layer of paratone-N oil, mounted on the diffractometer, and flash cooled to 100 K in the cold stream of the Cryojet XL liquid nitrogen cooling device (Oxford Instruments) attached to the diffractometer. The diffractometer was equipped with two sealed-tube long fine focus X-ray sources (Mo target, $\lambda = 0.71073$ Å; Cu target, $\lambda = 1.5418$ Å), a four-circle kappa goniometer, and an Atlas CCD detector. CrysAlisPro [20] software was used to control the diffractometer and perform data reduction and preliminary analysis. The crystal structure was solved with SHELXS [21]. All non-hydrogen atoms appeared in the E-map of the correct solution. Alternate cycles of model-building in Olex2 [22] and refinement in SHELXL [21] followed. All non-hydrogen atoms were refined anisotropically. All hydrogen atom positions were calculated based on idealized geometry, and recalculated after each cycle of least squares. During refinement, hydrogen atom – parent atom vectors were held fixed (riding motion constraint).

5. Synthetic details

5.1. 3,3′-dibromo-4,4′-bipyridine [10]

To a solution of 2.56 g diisopropylamine (25.3 mmol) in 50 mL tetrahydofuran, 15.8 mL of 1.6 M n-butyl lithium (25.3 mmol) was added dropwise at −90 °C. The solution was stirred at this temperature for 45 min. 4.0 g 3-bromopyridine (25.3 mmol) was added dropwise and allowed to stir for 1 h. 8.0 g $CuCl_2$ (59.5 mmol) was added, air was allowed into the reaction vessel, and the mixture was slowly warmed to room temperature and stirred overnight. The resulting brown solid was taken up in a mixture of 30 mL H_2O, 15 mL 30% w/w NH_4OH, and 15 mL saturated NH_4Cl then extracted three times with chloroform. The combined organic phases were dried with $NaSO_4$ and the volatiles removed under vacuum. The crude product was purified by column chromatography on silica gel (hexanes/ethyl acetate 2:1) to yield 1.23 g (31%) of 3,3′-dibromo-4,4′-bipyridine as off-white crystals.

5.2. 9,9-dimethyl-9H-silolo[2,3-c:5,4-c′]dipyridine (**1**) [9]

To a solution of 1.0 g 3,3′-dibromo-4,4′-bipyridine (3.18 mmol) in 40 mL THF was added 4.0 mL 1.6 M n-butyl lithium (6.4 mmol) dropwise at −90 °C. The mixture was stirred at this temperature for 1 h at 0.5 mL $SiMe_2Cl_2$ (4 mmol) was added dropwise and the mixture was allowed to warm to room temperature and stir overnight. The mixture was taken up in 50 mL 1 M $NaHCO_3$ and extracted three times with diethyl ether. The combined organic layers were dried over $MgSO_4$ and evaporated under vacuum to yield a light brown oil. The crude product was purified by column chromatography (SiO_2, hexanes/ethyl acetate, 1:2) followed by recrystallization from hexanes to yield **1** as colorless crystals (0.33 g, 49% yield). Crystals suitable for single-crystal X-ray analysis were grown via slow evaporation of a filtered diethyl ether solution at room temperature. ^1H NMR ($CDCl_3$, 300 MHz): $\delta = 8.90$ (s, 2 H), 8.75 (d, 2 H), 7.76 (d, 2 H) 0.56 (s, 6 H). $^{13}C\{^1H\}$ NMR ($CDCl_3$, 75 MHz): $\delta = 153.9$, 153.1, 151.7, 133.3, 116.9, −3.47 ppm. ^{29}Si NMR ($CDCl_3$, 60 MHz): $\delta = 3.62$ ppm. MS (EI): $m/z = 212.1$ (M^+), 197.1 ($[M-CH_3]^+$).

5.3. N,N′,Si,Si′-tetramethylsilanoviologen triflate (**2**)

To a solution of **1** (0.5 g, 2.4 mmol) in acetonitrile (20 mL) was added methyl triflate (0.79 g, 4.8 mmol) dropwise at 0 °C. The solution was stirred overnight and diethyl ether allowed to slowly diffuse into the reaction vessel, yielding the tetramethylsilanoviologen, **2**, as colorless needles (0.78 g, 61% yield). Crystals suitable for single-crystal X-ray analysis were grown via slow ether diffusion into a saturated acetonitrile solution under a nitrogen atmosphere. ^1H NMR ($CDCl_3$, 300 MHz): $\delta = 9.06$ (s, 2 H), 8.83 (d, 2 H), 8.61 (d, 2 H), 4.36 (s, 6 H) 0.70 (s, 6 H). $^{13}C\{^1H\}$ NMR ($CDCl_3$, 75 MHz): $\delta = 157.2$, 151.0, 148.7, 142.4, 123.9, 49.5, −4.58 ppm. ^{29}Si NMR ($CDCl_3$, 60 MHz): $\delta = 10.0$ ppm. *Anal.* Calc. (%) for $C_{16}H_{18}N_2O_6F_6SiS_2$: C, 35.55, H, 3.36, N, 5.18. Found: C, 35.38, H, 3.19, N, 5.20%. MS (MALDI-TOF): $m/z = 242.5$ (M^+), 227.6 ($[M-CH_3]^+$).

5.4. Ring-opening hydrolysis product of the silanoviologen (formation of **3**)

To a solution of 25 mg **1** (0.12 mmol) in 1 mL CD_3CN was added 34 mg CH_3I (0.24 mmol). The mixture was allowed to stand overnight, resulting in a red precipitate. The supernatant was decanted and allowed to slowly evaporate in air to yield crystals of the hydrolyzed compound **3** which were suitable for single-crystal

X-ray analysis. NMR data (triflate salt): ^{1}H NMR (D_2O, 300 MHz): δ = 9.01 (m, 2 H), 8.94 (m, 2 H), 8.21 (d, 1 H), 8.02 (d, 1 H) 4.51 (s, 3 H), 4.47 (s, 3 H), 2.22 (s, 1 H), 0.33 (s, 6H).

Acknowledgement

The authors gratefully acknowledge financial support of this research from the UNC Charlotte Faculty Research Grant Program.

Appendix A. Supplementary data

Supplementary data associated with this article can be found, in the online version, at http://dx.doi.org/10.1016/j.poly.2017.05.040.

References

[1] (a) For recent reviews see: A.J. Esswein, D.G. Nocera Chem. Rev. 107 (2007) 4022;
(b) S. Fukuzumi, Eur. J. Inorg. Chem. (2008) 1351;
(c) Y. Amao, ChemCatChem 3 (2011) 458.
[2] S.E. Chun, B. Evanko, X.F. Wang, D. Vonlanthen, X.L. Ji, G.D. Stucky, S.W. Boettcher, *Nat. Commun.* 6 (2015) 7818.
[3] R.J. Mortimer, Annu. Rev. Mater. Res., in: D.R. Clarke, P. Fratzl (Eds.) 41 (2011) 241.
[4] C.L. Bird, A.T. Kuhn, Chem. Soc. Rev. 10 (1981) 49.
[5] (a) J. Liu, J.W.Y. Lam, B.Z. Tang, J. Inorg. Organomet. Polym. 19 (2009) 249;
(b) G. Lu, H. Usta, C. Risko, L. Wang, A. Facchetti, M.A. Ratner, T.J. Marks, J. Am. Chem. Soc. 130 (2008) 7670;
(c) M. Saito, M. Yoshioka, Coord. Chem. Rev. 249 (2005) 765;
(d) G. Yu, S.W. Yin, Y.Q. Liu, J.S. Chen, X.J. Xu, X.B. Sun, D.G. Ma, X.W. Zhan, Q. Peng, Z.G. Shuai, B.Z. Tang, D.B. Zhu, W.H. Fang, Y. Luo, J. Am. Chem. Soc. 127 (2005) 6335.
[6] (a) T.Y. Chu, J.P. Lu, S. Beaupre, Y.G. Zhang, J.R. Pouliot, S. Wakim, J.Y. Zhou, M. Leclerc, Z. Li, J.F. Ding, Y. Tao, J. Am. Chem. Soc. 133 (2011) 4250;
(b) J.W. Chen, Y. Cao, Acc. Chem. Res. 42 (2009) 1709;
(c) J.H. Hou, H.Y. Chen, S.Q. Zhang, G. Li, Y. Yang, J. Am. Chem. Soc. 130 (2008) 16144.
[7] (a) H. Sohn, M.J. Sailor, D. Magde, W.C. Trogler, J. Am. Chem. Soc. 125 (2003) 3821;
(b) S.J. Toal, W.C. Trogler, J. Mater. Chem. 16 (2006) 2871.
[8] J.W. Chen, Y. Cao, Macromol. Rapid Commun. 28 (2007) 1714.
[9] J. Ohshita, K. Murakami, D. Tanaka, Y. Ooyama, T. Mizumo, N. Kobayashi, H. Higashimura, T. Nakanish, Y. Hasegawa, Organometallics 33 (2014) 517.
[10] S. Durben, T. Baumgartner, Angew. Chem. Int. Ed. 50 (2011) 7948.
[11] (a) M. Stolar, J. Borau-Garcia, M. Toonen, T. Baumgartner, J. Am. Chem. Soc. 137 (2015) 3366. (b) C. Reus, M. Stolar, J. Vanderkley, J. Nebauer, T. Baumgartner, J. Am. Chem. Soc., 137 (2015) 11710.
[12] A. Launikonis, A.W.H. Mau, W.H.F. Sasse, L.A. Summers, J. Chem. Soc., Chem. Commun. (1986) 1645.
[13] L. Kaczmarek, B. Pol, Acad. Sci. Chem. 35 (1987) 269.
[14] K. Murakami, J. Ohshita, S. Inagi, I. Tomita, Electrochemistry 83 (2015) 605.
[15] R.N. Dominey, T.J. Lewis, M.S. Wrighton, J. Phys. Chem. 87 (1983) 5345.
[16] S.Y. Choi, M. Mamak, N. Coombs, N. Chopra, G.A. Ozin, Nano Lett. 4 (2004) 1231.
[17] G.D. Watt, Renew. Energy 72 (2014) 99.
[18] T. Watanabe, K. Honda, J. Phys. Chem. 86 (1982) 2617.
[19] J. Peon, X. Tan, J.D. Hoerner, C.G. Xia, Y.F. Luk, B. Kohler, J. Phys. Chem. A 105 (2001) 5768.
[20] Agilent Technologies (2012). Agilent Technologies UK Ltd., Oxford, UK, Xcalibur/SuperNova CCD system, CrysAlisPro Software system, Version 1.171.36.28.
[21] G.M. Sheldrick, Acta Cryst. A64 (2008) 112.
[22] O.V. Dolomanov, L.J. Bourhis, R.J. Gildea, J.A.K. Howard, H. Puschmann, *J. Appl. Cryst.* 42 (2009) 339.